

Electronic Supplementary Information (ESI)

**3D nitrogen doped hierarchical porous carbon framework for
protecting sulfur cathode in lithium sulfur batteries**

Yan Song, He Wang, Qianli Ma, Dan Li, Jinxian Wang, Guixia Liu, Ying Yang, Xiangting Dong*,
and Wensheng Yu*

School of Chemistry and environmental engineering, Changchun University of Science and
Technology, Changchun 130022, China.

*corresponding authors: E-mail: dongxiangting888@163.com, wenshengyu2009@sina.com

Supplementary Figures

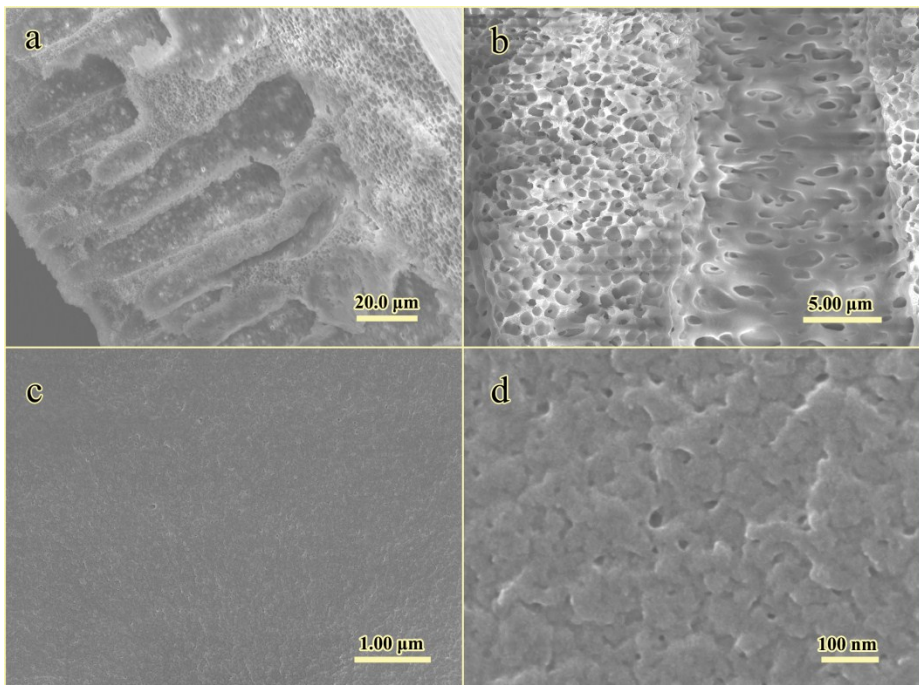


Fig. S1 Morphological features of (a, b) cross-section and (c, d) surface of the hierarchical porous PAN framework.

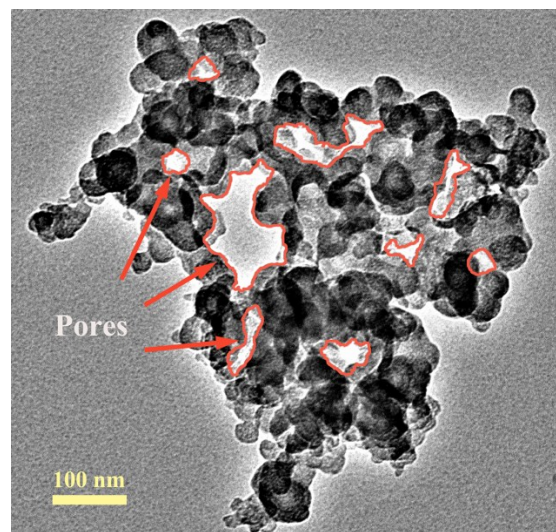


Fig. S2 Transmission electron microscopy (TEM) image of the NHPCF.

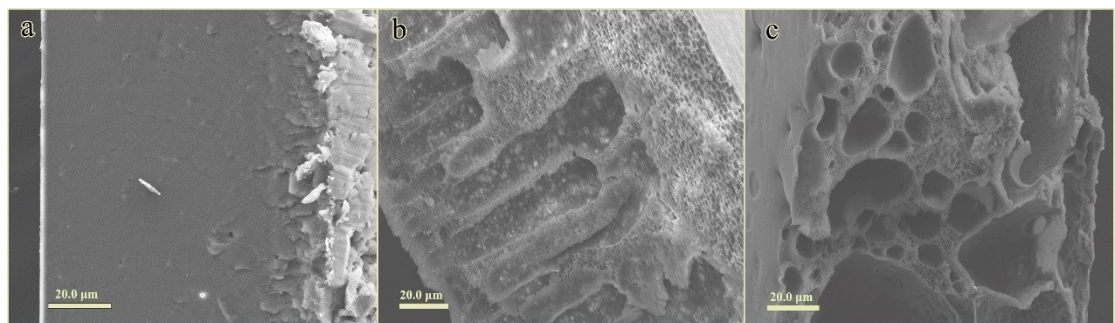


Fig. S3 Field-emission scanning electron microscopy (FE-SEM) images of the PAN framework at different ratio of PAA to PAN in the precursor (a. 0:1, b. 1:2, c.1:1).

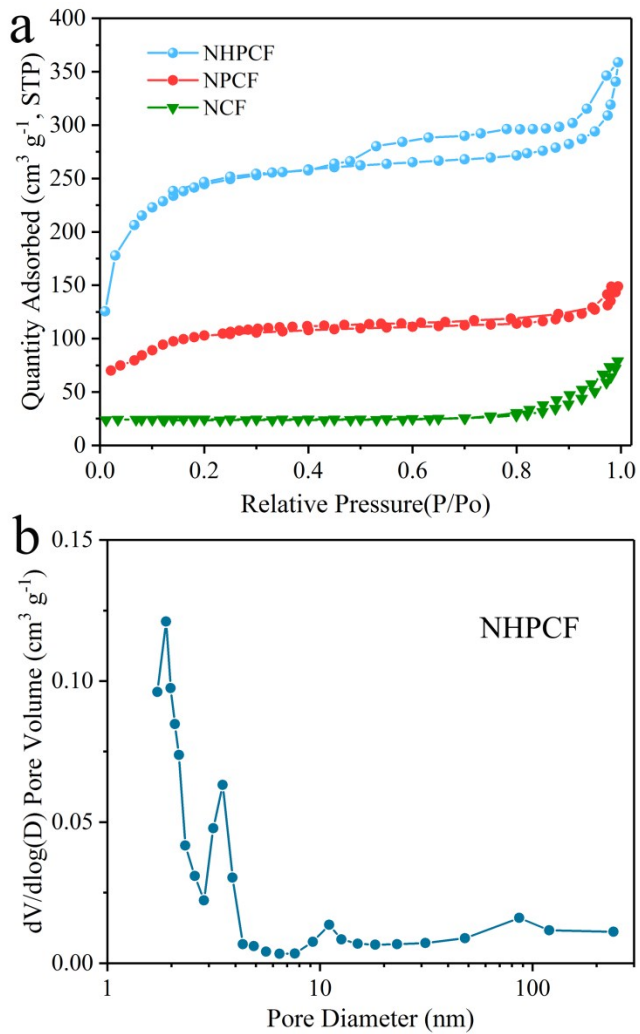


Fig. S4 (a) N_2 adsorption/desorption isotherms of NHPCF, NPCF, and NCF sample; (b) pore size distributions for NHPCF.

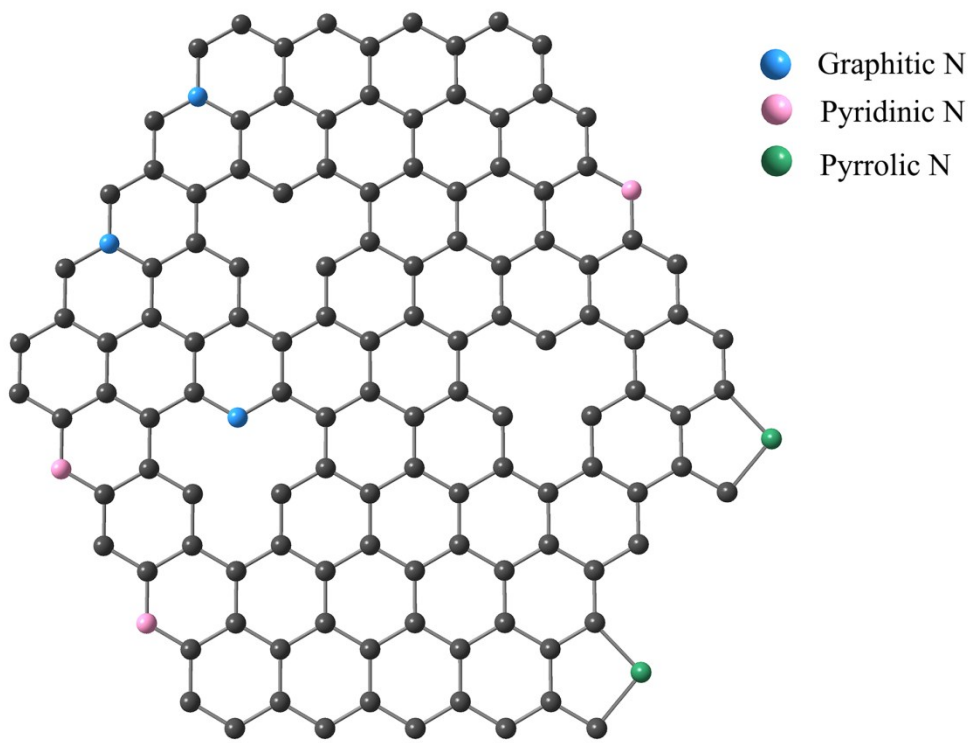


Fig. S5 Schematic configuration of NHPCF with various nitrogen atoms.

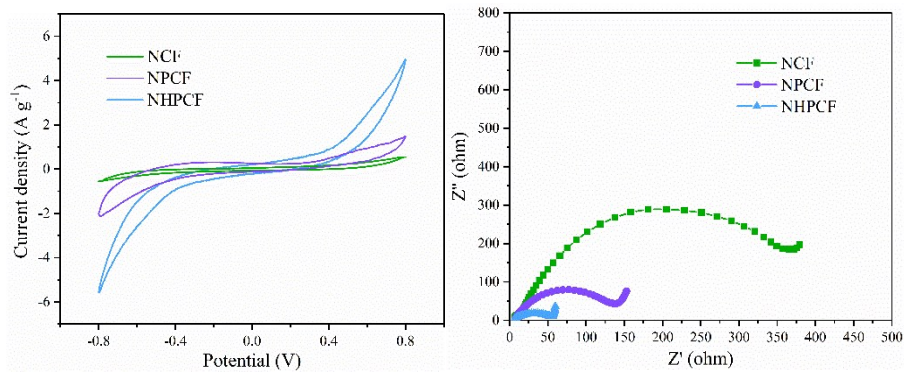


Fig. S6 (a) cyclic voltammetry curves and (b) electrochemical impedance spectra of symmetric batteries with two identical electrodes and the electrolyte containing Li_2S_6 (0.5 M)

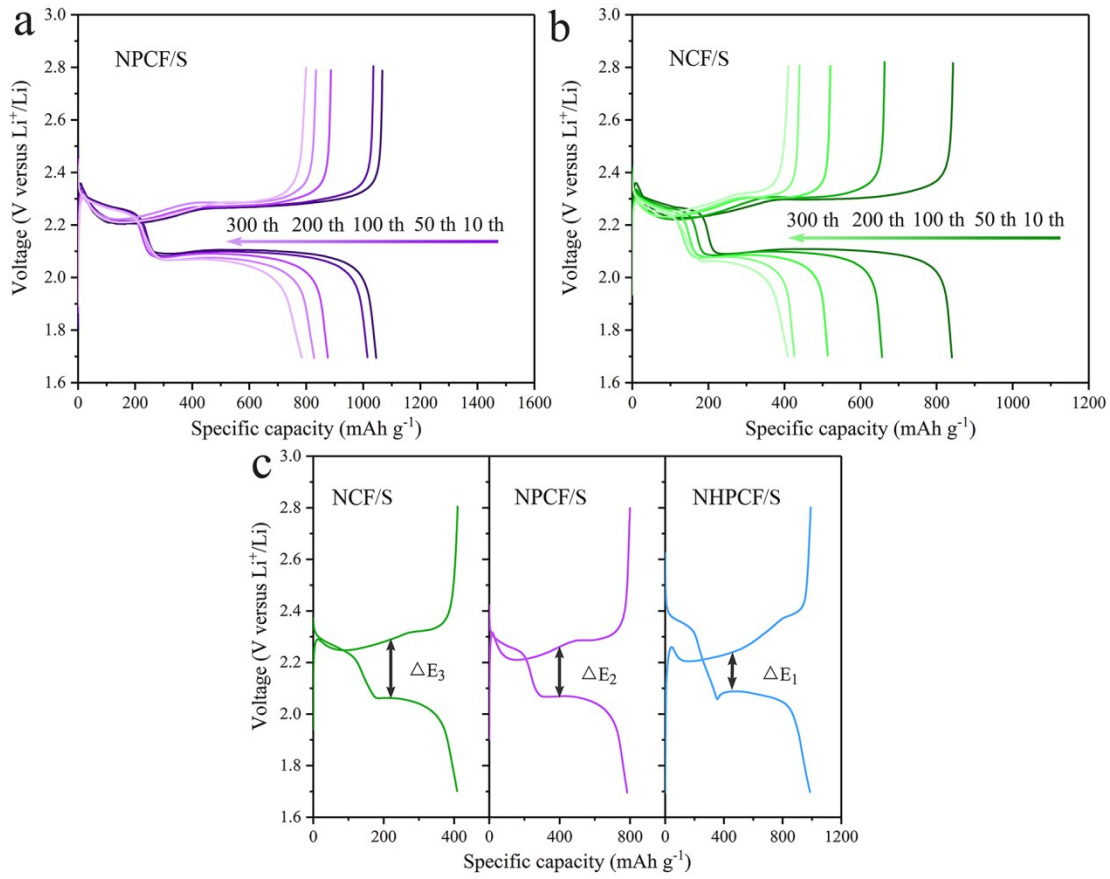


Fig. S7 Galvanostatic discharge-charge curves of different cycles for (a) NPCF/S and (b) NCF/S cathodes at 0.1 C, (c) the 300th discharge-charge curves of the cells with NCF/S, NPCF/S, and NHPCF/S cathodes.

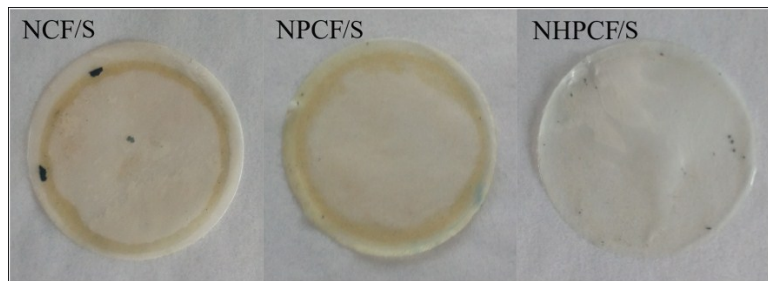


Fig. S8 Photographs of the separators of cells with NCF/S, NPCF/S, and NHPCF/S electrodes after 300 cycles at 0.1 C.

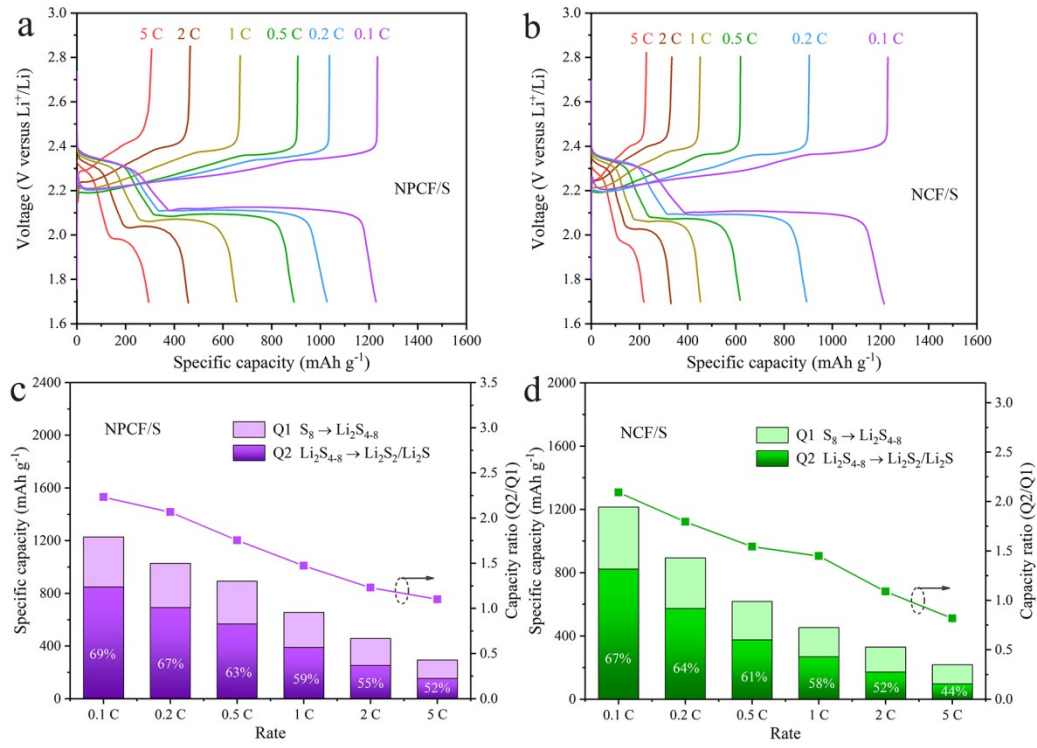


Fig. S9 Galvanostatic discharge-charge voltage profiles of the cells with (a) NPCF/S and (b) NCF/S cathodes at different current rates. Corresponding capacity contribution of the two discharge stages for the cells with (c) NPCF/S and (d) NCF/S cathodes at different current rates.

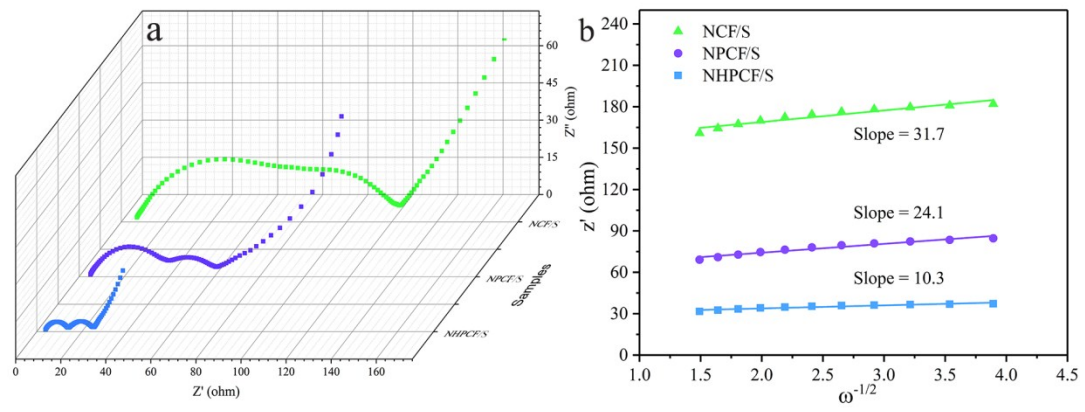


Fig. S10 (a) Nyquist and (b) Warburg plots of NCF/S, NPCF/S, and NHPCF/S electrode after cycling.

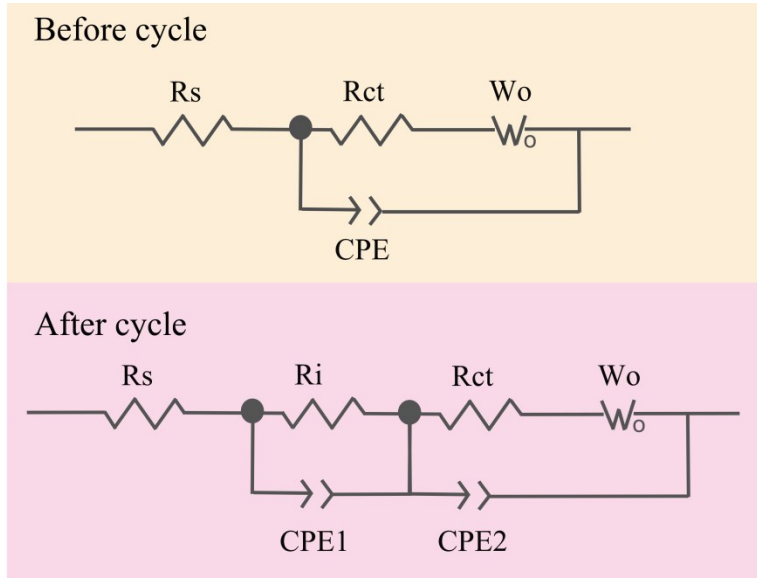


Fig. S11 Equivalent circuit models of the cell before and after charge-discharge cycle. (R_s : the resistance of the electrolyte; R_i : the resistance of the insoluble $\text{Li}_2\text{S}_2/\text{Li}_2\text{S}$ layer; R_{ct} : the charge-transfer resistance; CPE: the corresponding constant phase element; W_o : the semi-infinite Warburg diffusion impedance.)

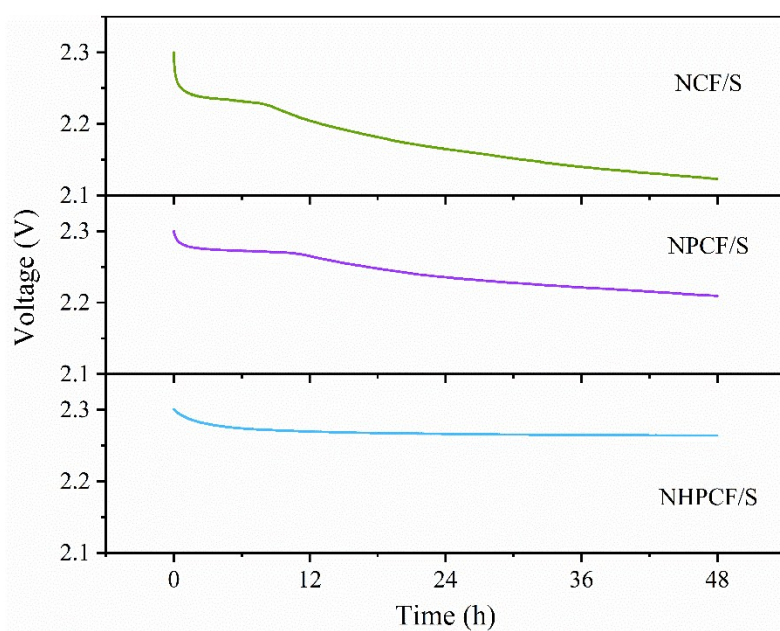


Fig. S12 Open circuit voltage of the cells with NCF/S, NPCF/S, and NHPCF/S electrode during the battery rest after charging to 2.3 V.

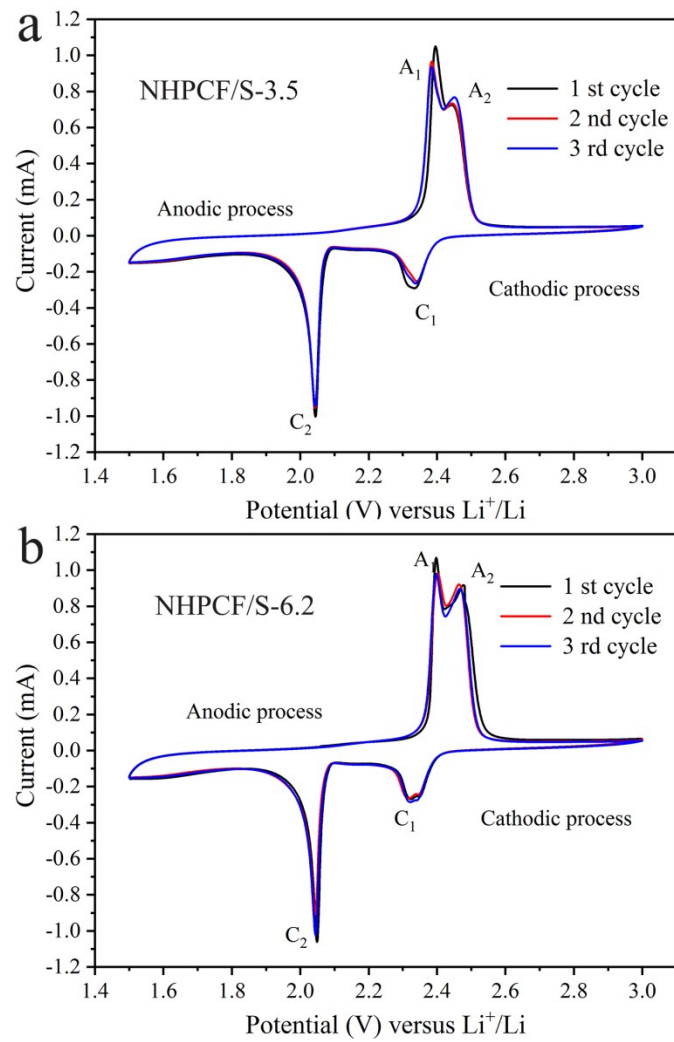


Fig. S13 CV curves of NHPCF/S with high sulfur loading of (a) 3.5 and (b) 6.2 mg cm⁻².

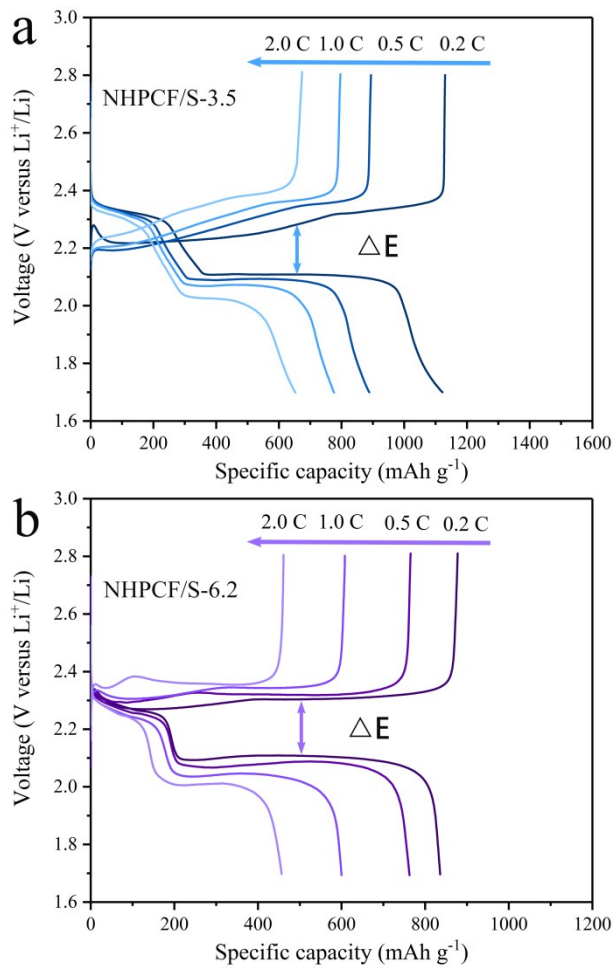


Fig. S14 Galvanostatic discharge–charge voltage profiles of NHPCF/S with high sulfur loading of (a) 3.5 and (b) 6.2 mg cm^{-2} .

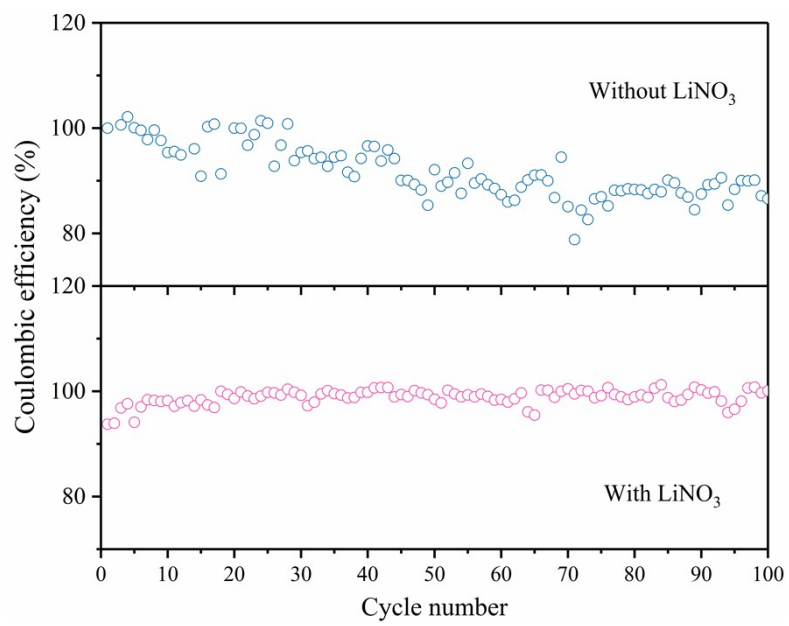


Fig. S15 Coulombic efficiency of the cells with and without LiNO₃ containing electrolyte at rate of 1.0 C.

Supplementary Table

Table S1 Performance comparisons of present work with reported porous carbon host for Li-S battery.

Host	Sulfur loading (mg cm ⁻²)	Capacity (mAh g ⁻¹)/Rate	Capacity retention (mAh g ⁻¹)	Cycle number	Decay rate per cycle (%)	Ref.
Porous carbon		1200/0.2 C	872	100	0.29	¹
Hierarchical porous carbon		1265/500 mA g ⁻¹	643	50	0.98	²
Microporous bamboo carbon	1.0	961/800 mA g ⁻¹	550	150	0.29	³
Hierarchical micro-/mesopores carbon materials	1.0	834/0.5 C 658/1 C	600 586	500 200	0.056 0.055	⁴
Three-dimensional porous graphitic carbon	2.36	1242/1 C	917	200	0.13	⁵
3D graphene nanosheet@carbon nanotube	1.3-1.6	1373.8/0.1 C	836.5	200	0.20	⁶
3D graphene Frameworks	1.5	521/1 C	305	500	0.107	⁷
Three-dimensional metal carbide MXene/reduced graphene oxide hybrid nanosheets	1.5	1144.2/0.5 C	878.4	300	0.077	⁸
Three dimensional porous cellular carbon framework	1.4-1.6	1108/0.1 C	917.2	100	0.17	⁹
N-doped porous carbon microspheres	1.1-1.3	1119.5/0.1 A g ⁻¹	1030.7	100	0.079	¹⁰
Hierarchical porous N, O dual doped carbon microrods	1.2	1327/0.2C	1071	160	0.082	¹¹
Nitrogen-rich mesoporous carbon	0.7-1.0	1291/0.5 C	643	200	0.25	¹²
3D nitrogen doped hierarchical porous carbon framework	2.0 6.5	1228/0.1 C 650/1 C	1000 425	300 500	0.06 0.069	This work

References

- 1 K. Yang, Q. Gao, Y. Tan, W. Tian, W. Qian, L. Zhu and C. Yang, *Chem.- Eur. J.*, 2016, **22**, 3239.
- 2 S. Wei, H. Zhang, Y. Huang, W. Wang, Y. Xia and Z. Yu, *Energy Environ. Sci.*, 2011, **4**, 736.
- 3 X. Gu, Y. Wang, C. Lai, J. Qiu, S. Li, Y. Hou, W. Martens, N. Mahmood and S. Zhang, *Nano Res.*, 2015, **8**, 129.
- 4 M. K. Rybarczyk, H.-J. Peng, C. Tang, M. Lieder, Q. Zhang and M.-M. Titirici, *Green Chem.*, 2016, **18**, 5169.
- 5 G. Li, J. Sun, W. Hou, S. Jiang, Y. Huang and J. Geng, *Nat. Commun.*, 2016, **7**, 10601.
- 6 Z. Zhang, L. Kong, S. Liu, G. Li and X. Gao, *Adv. Energy Mater.*, 2017, **7**, 1602543.
- 7 J. Cai, Z. Zhang, S. Yang, Y. Min, G. Yang and K. Zhang, *Electrochim. Acta*, 2019, **295**, 900.
- 8 W. Bao, X. Xie, J. Xu, X. Guo, J. Song, W. Wu, D. Su and G. Wang, *Chem.- Eur. J.*, 2017, **23**, 12613.
- 9 Y. Wang, S. Luo, D. Wang, X. Hong and S. Liu, *Electrochim. Acta*, 2018, **284**, 400.
- 10 Y. Xia, R. Fang, Z. Xiao, H. Huang, Y. Gan, Y. Yan, X. Lu, C. Liang, J. Zhang, X. Tao and W. Zhang, *ACS Appl. Mater. Interfaces*, 2017, **9**, 23782.
- 11 N. Wang, Z. Xu, X. Xu, T. Liao, B. Tang, Z. Bai and S. Dou, *ACS Appl. Mater. Interfaces*, 2018, **10**, 13573.
- 12 Y. Qu, Z. Zhang, X. Zhang, G. Ren, Y. Lai, Y. Liu and J. Li, *Carbon* 2015, **84**, 399.